Novel mRNA-containing cytoplasmic granules in ALK-transformed cells

Mohamad Fawal[a,*], Olivier Jean-Jean[b], Nathalie Vanzo[a], and Dominique Morello[a]
[a]CNRS-UMR 5547, IFR 109, Université Paul Sabatier, 31062 Toulouse, France; [b]UPMC Univ Paris 06, CNRS-FRE 3402, 75005 Paris, France

ABSTRACT **In mammalian cells, nontranslating messenger RNAs (mRNAs) are concentrated in different cytoplasmic foci, such as processing bodies (PBs) and stress granules (SGs), where they are either degraded or stored. In the present study, we have thoroughly characterized cytoplasmic foci, hereafter called AGs for ALK granules that form in transformed cells expressing the constitutively active anaplastic lymphoma kinase (ALK). AGs contain polyadenylated mRNAs and a unique combination of several RNA binding proteins that so far has not been described in mammalian foci, including AUF1, HuR, and the poly (A+) binding protein PABP. AGs shelter neither components of the mRNA degradation machinery present in PBs nor known markers of SGs, such as translation initiation factors or TIA/TIAR, showing that they are distinct from PBs or SGs. AGs and PBs, however, both move on microtubules with similar dynamics and frequently establish close contacts. In addition, in conditions in which mRNA metabolism is perturbed, AGs concentrate PB components with the noticeable exception of the 5′ to 3′ exonuclease XRN1. Altogether, we show that AGs constitute novel mRNA-containing cytoplasmic foci and we propose that they could protect translatable mRNAs from degradation, contributing thus to ALK-mediated oncogenicity.**

Monitoring Editor
Marvin P. Wickens
University of Wisconsin

Received: Jul 6, 2010
Revised: Dec 22, 2010
Accepted: Jan 5, 2011

INTRODUCTION

A key aspect of gene regulation in eukaryotes is the cytoplasmic control of messenger RNA (mRNA) degradation and translation. A number of cytoplasmic granules containing messenger ribonucleoproteins (mRNPs) have been identified in the past few years, including stress granules (SGs; Anderson and Kedersha, 2009), neuronal granules (Kiebler and Bassell, 2006), germ cell specific granules (Seydoux and Braun, 2006), and processing bodies (PBs; reviewed in Eulalio *et al.*, 2007; Franks and Lykke-Andersen, 2008; Balagopal and Parker, 2009; Moser and Fritzler, 2009; Kulkarni *et al.*, 2010). PBs, also known as GW bodies, are involved in the deadenylation-decapping-5′-3′ decay pathway as well as in microRNA-mediated silencing, non–sense-mediated mRNA decay, and AU-rich mRNA decay (AMD) (review in Eulalio *et al.*, 2007; Garneau *et al.*, 2007; Franks and Lykke-Andersen, 2008; Kulkarni *et al.*, 2010). It is still questionable whether mRNA decay happens within PBs. However, the fact that they concentrate decapping enzymes (DCP1a-b and DCP2), activators of decapping (LSM1–7, RCK/p54, EDC1–3), and the 5′ to 3′ exonuclease XRN1 but neither ribosomal proteins nor most of the translation factors strongly suggests that PBs are active sites of mRNA degradation (Cougot *et al.*, 2004; Sheth and Parker, 2006). PBs, however, have also been shown to be storage sites for translationally arrested mRNAs that can return to translation (Brengues *et al.*, 2005; Teixeira *et al.*, 2005; Bhattacharyya *et al.*, 2006; Sheth and Parker, 2006).

Mammalian cells also contain cytoplasmic foci that appear in response to environmental stresses and are thus called SGs (reviewed in Anderson and Kedersha, 2008). SGs accommodate mRNAs, proteins of the small ribosomal subunit, several translation

This article was published online ahead of print in MBoC in Press (http://www.molbiolcell.org/cgi/doi/10.1091/mbc.E10-07-0569) on January 13, 2011.

Author contributions: M. Fawal conceived and performed the experiments, analyzed the data, and prepared the digital images; O. Jean-Jean and D. Morello conceived experiments, analyzed the data, and drafted the article; and N. Vanzo drafted the article.

*Present address: Centro Nacional de Investigaciones Oncológicas (CNIO)/Spanish National Cancer Research Centre, Melchor Fernández Almagro, 3. 28029 Madrid, Spain.

Address correspondence to: Dominique Morello (morello@cict.fr).

Abbreviations used: ActD, actinomycin D; AG, ALK granule; ALCL, anaplastic large cell lymphomas; ALK, anaplastic lymphoma kinase; AMD, AU-rich mRNA decay; ATIC, 5-aminoimidazole-4-carboxamide ribonucleotide formyltransferase/IMP cyclohydrolase; AU-BP, AU-binding protein; CHX, cycloheximide; EtBr, ethidium bromide; mRNA, messenger RNA; mRNP, messenger ribonucleoprotein; NMP, nucleophosmin; PABP, poly (A+) binding protein; PB, processing body; SG, stress granule; TPM3, tropomyosin 3; YFP, yellow fluorescent protein.

initiation factors (Kedersha *et al.*, 2002, 2005), poly (A^+) binding protein (PABP; Kedersha *et al.*, 1999), and repressors of translation, such as TIA/TIAR (Piecyk *et al.*, 2000) and CPEB1 (Wilczynska *et al.*, 2005), as well as other components, including the AU-binding protein (AU-BP) HuR (Gallouzi *et al.*, 2000). As SGs do not include components of the mRNA degradation machinery, these granules are believed to be sites of mRNA storage (reviewed in Anderson and Kedersha, 2009). Although SGs and PBs are clearly distinct structures, they share proteins, in particular TTP and BRF1, two AU-BPs involved in AMD (Fenger-Gron *et al.*, 2005; Franks and Lykke-Andersen, 2007), and the same reporter mRNA (Kedersha *et al.*, 2005), leading to the proposal that PBs and SGs might exchange mRNPs (Balagopal and Parker, 2009). The recent observation that PBs and SGs move within the cytoplasm in a microtubule-dependent manner gives support to this hypothesis (Aizer and Shav-Tal, 2008; Chernov *et al.*, 2009; Nadezhdina *et al.*, 2010) and strongly suggests that cycling of mRNPs among polysomes, PBs, and SGs requires an intact microtubule network.

Studying nucleophosmin-anaplastic lymphoma kinase (NPM-ALK)-transformed cells, we and others have recently detected cytoplasmic foci that concentrate this oncogenic tyrosine kinase (Fawal *et al.*, 2006; Honorat *et al.*, 2006). NMP-ALK is a chimeric protein resulting from the (t2;5)(p23;q35) chromosomal translocation bringing the *NPM* gene at 5q35 in juxtaposition with the *ALK* gene at 2p23, which encodes a receptor tyrosine kinase expressed almost exclusively in the CNS during embryogenesis (Morris *et al.*, 1997). Even though *NPM-ALK* is the most frequent chromosomal translocation observed in anaplastic large cell lymphomas (ALCLs; Morris *et al.*, 1997; Pulford *et al.*, 1997; Benharroch *et al.*, 1998), other less common N-terminal–fused partners of ALK, such as ATIC (5-aminoimidazole-4-carboxamide ribonucleotide formyltransferase/IMP cyclohydrolase) or TPM3 (tropomyosin 3), have been described (Lamant *et al.*, 1999; Touriol *et al.*, 2000; Trinei *et al.*, 2000). In those cases, the N-terminal partners of ALK share an oligomerization domain triggering the constitutive autophosphorylation of ALK and activation of its oncogenic properties (Pulford *et al.*, 2004a). In turn, various signaling pathways are activated (Bai *et al.*, 2000; Zamo *et al.*, 2002), leading to unregulated growth of X-ALK–expressing cells (Duyster *et al.*, 2001; Pulford *et al.*, 2004b).

Searching for NPM-ALK interacting partners, we found that AUF1/hnRNPD, a protein implicated in AMD (Zhang *et al.*, 1993; Bevilacqua *et al.*, 2003), was immunoprecipitated with NPM-ALK, both in ALCL–derived cell lines and in NIH3T3 cells stably expressing NPM-ALK that recapitulate most of the tumorigenic properties of ALCLs (Armstrong *et al.*, 2004). In addition to their localization in the nucleus, both NPM-ALK and AUF1 were found to concentrate within discrete cytoplasmic foci in NPM-ALK–expressing NIH3T3 and ALCL-derived cells (Fawal *et al.*, 2006; Honorat *et al.*, 2006). We also found that several AUF1-target mRNAs encoding key regulators of cell proliferation are stabilized in these cells, giving those cells a survival advantage that could contribute to their oncogenic properties (Fawal *et al.*, 2006). We thus hypothesized that NPM-ALK cytoplasmic bodies, hereafter called AGs (for ALK granules), could act to control cytoplasmic mRNA fate. In this work, we have further characterized AGs. We show that they concentrate the active, phosphorylated form of NPM-ALK. They do contain mRNAs but do not include components of mRNA translation or degradation machineries. Using live cell imaging, we have visualized the dynamics of AGs in the cytoplasm and found it similar to that of PBs. Indeed, most AGs are mobile and require an intact microtubule network for their movement. Altogether, our results highlight an unexpected function of cytoplasmic NPM-ALK in assembling large mRNP structures. We propose that through their ability to scan the cytoplasm and capture mRNAs, AGs may be potent actors of cell transformation.

RESULTS

X-ALK fusion proteins are concentrated in cytoplasmic foci in their active phosphorylated form

In cells derived from ALCLs, NPM-ALK is expressed in the nucleus, including nucleolus (Pulford *et al.*, 1997) and in small cytoplasmic foci (AGs) (Fawal *et al.*, 2006; Honorat *et al.*, 2006). AGs are also detected in NPM-ALK expressing NIH3T3 cells (Fawal *et al.*, 2006, and Figure 1A, left) that are used as a convenient model to study NPM-ALK oncogenic properties (Armstrong *et al.*, 2004). In those cells, NPM-ALK expression is weaker than in ALCL-derived cell lines (Figure 1B), showing that AG nucleation does not result from aberrant NPM-ALK overexpression. Most NPM-ALK NIH3T3 cells and the two ALCL-derived cell lines, Cost and Karpas, contain AGs with an average of 8 cytoplasmic foci per cell (see Figure 1A, Supplemental Figures S1A for quantification and S4B for Karpas AGs). Such cytoplasmic foci were not observed in NIH3T3 cells transiently transfected with vector encoding NPM-enhanced green fluorescent protein (eGFP) (Grummitt *et al.*, 2008) or the full-length ALK receptor (Figure S1B), showing that NPM-ALK fusion is required for AG nucleation. We previously established that a kinase dead mutant of NPM-ALK protein could not nucleate AGs (Fawal *et al.*, 2006). Consistent with this result, we observed that AGs disappear when NPM-ALK NIH3T3 cells are treated with an ALK specific inhibitor (see *Materials and Methods*) that does not modify the level of NPM-ALK but inhibits its kinase activity (Figures 1C and S1B).

To test whether other ALK fusions nucleate AGs, we stained previously described TPM3- and ATIC-ALK NIH3T3 cells (Armstrong *et al.*, 2004) with anti-ALK and anti-phospho-ALK antibodies. Confocal microscopy analysis showed that both cell types concentrate the ALK fusion proteins in cytoplasmic foci in their phosphorylated (i.e., active kinase form; Figure 1A and data not shown for ATIC-ALK). Altogether, these results indicate that ALK is present in its phosphorylated form in AGs and that AG formation relies on the active tyrosine kinase domain of ALK fusions.

AGs contain polyadenylated mRNAs

It is well established that cytoplasmic foci such as PBs and SGs accumulate mRNAs together with mRNA-binding proteins. As AGs contain the RNA-binding protein AUF1 (Fawal *et al.*, 2006), we further asked whether AGs also contained mRNAs. First, to test this hypothesis, we used ethidium bromide (EtBr) to fluorescently label endogenous RNAs in NPM-ALK NIH3T3 cells, as previously described (Tang *et al.*, 2001). When cells were simultaneously stained with anti-ALK antibodies, we observed that ~50% of ALK-containing cytoplasmic foci also concentrate EtBr (Figure 2A). Second, PABP was detected in AGs of NPM-ALK 3T3 cells stained both with anti-PABP and anti–phospho-ALK antibodies (Figure 2B). Those results were indicative of the presence of mRNAs in AGs. To directly test this hypothesis, we transiently expressed both a lacZ reporter mRNA containing MS2-binding sites in its 3′ untranslated region (lacZ-3′MS2) and a yellow fluorescent protein (YFP)-MS2 fusion protein. When expressed alone, the YFP-MS2 protein was found exclusively in the nucleus, due to its nuclear localization signal (Rook *et al.*, 2000). In contrast, coexpressing lacZ- 3′MS2 mRNA and YFP-MS2 allowed YFP-MS2 tethering to lacZ-3′MS2 mRNA and its subsequent export from the nucleus to the cytoplasm where it concentrates in PBs (Kedersha *et al.*, 2005). In NPM-ALK transformed NIH3T3cells, the reporter mRNA is both visualized in PBs revealed by anti-DCP1 antibody and, although at a weaker intensity (1.6-fold lower), in

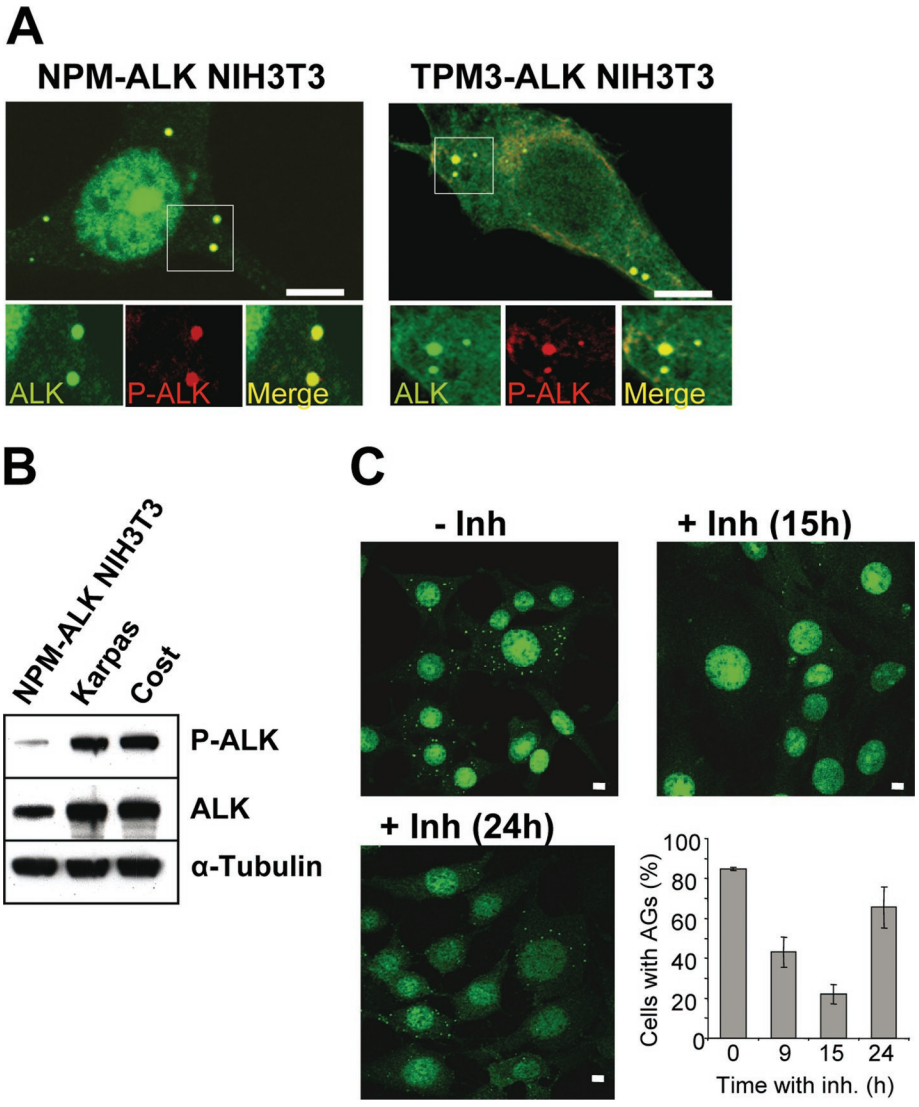

FIGURE 1: AGs correspond to cytoplasmic foci containing an active X-ALK kinase domain. (A) Confocal analysis of NIH3T3 cell lines stably expressing NPM- or TPM3-ALK using anti-ALK and anti-phospho ALK antibodies. The merge view shows localization of phosphorylated fusion-ALK proteins in AGs. (B) Western blot analysis of NPM-ALK level of expression in NPM-ALK NIH3T3 and ALCL-derived Karpas and Cost cell lines using anti-phospho (P-ALK) and anti-ALK (ALK) antibodies. (C) ALK inhibitor prevents ALK phosphorylation. NPM-ALK NIH3T3 cells were treated with the ALK inhibitor, fixed at different times after treatment, and analyzed for immunofluorescence using anti-ALK antibody with a wide-field microscope to determine the kinetics of the loss of AGs. Whereas 85% of untreated cells (0 h) contained more than one AG, there were only 22% at the peak of NPM-ALK dephosphorylation (15 h). Most probably due to the transient activity of the inhibitor and concomitant to NPM-ALK rephosphorylation (Supplemental Figure S1C), AGs reappear, and ~70% of cells contained AGs 24 h after treatment. Results shown were obtained in three independent experiments. The scale bar represents 5 μm.

most AGs (90%) with a diameter > 0.1 μm (Figure 2, C and D). These data are in agreement with our previous findings showing that PBs and AGs are distinct structures (Fawal *et al.*, 2006), and reveal that AGs and PBs can harbor the same mRNA species. Finally, to know whether mRNAs contained in AGs were polyadenylated, we performed in situ hybridization using oligo(dT) probe. Concomitant immunodetection of AGs using anti-phospho-ALK antibodies revealed that most large AGs (90%) contained both NPM-ALK and oligo(dT) (Figure 2E). All together, those different approaches show that AGs concentrate mRNAs that are polyadenylated.

AG formation and movements

To further characterize AG formation, we transiently expressed NPM-ALK as a GFP (NPM-ALK-GFP) or Halo (NPM-ALK-Halo) fusion protein in NIH3T3 cells. Those fusion proteins conserve their phosphorylation status as shown by Western blot analysis (Figure S2A) and nucleate cytoplasmic foci the number, shape, and size of which were identical to those observed in NPM-ALK stably transformed NIH3T3 cells (compare Figure S2B to Figures 1A and 6A later in the paper). We then visualized AG formation and movements in the cytoplasm conducting both short (2 min) and long term (24 h) time-lapse analysis to track AG movements, as previously described for PBs (Aizer and Shav-Tal, 2008). Using GFP-NPM-ALK transiently transfected cells, we observed that AGs rapidly grow to reach their standard size (0.3- to 0.5-μm diameter within 10 min) (Figure S2C). Single particle tracking from short-range movies (2 min, Supplemental Movie 1) allowed us to classify AGs into three categories according to their roamed distances: <5 μm, 5–10 μm or >10 μm (Figure 3, A, C, and D). The latter could be tracked for distances up to 18 μm (Figures 3 and S3). To compare AG and PB movements in the same cellular context, we transfected NIH3T3 cells with a GFP-DCP1a construct and observed similar tracking profiles for AGs and PBs, although AGs move globally slightly faster than PBs (Figures 3 and S3).

Owing to this similarity, we tested whether AGs could associate to the microtubule cytoskeleton, as recently described for PBs (Aizer and Shav-Tal, 2008). Using double staining with anti–α-tubulin and anti-ALK antibodies, we observed AGs decorating individual microtubule bundles in NPM-ALK NIH3T3 cells (Figure 4A), suggesting that AG movements rely on their association with microtubules. This hypothesis was tested by treating cells with nocodazole, which binds to tubulin monomers and leads to microtubule destabilization. NIH3T3 cells were transiently transfected with NPM-ALK-GFP, and AG movements were observed before and after microtubule disruption. Short-range time-lapse analysis indicates that nocodazole significantly reduces AG mobility (compare Figure 4B to Figures 3C and 4C for statistical analysis). Comparison with PBs observed in GFP-DCP1a–expressing NIH3T3 cells shows that nocodazole treatment inhibits both AG and PB movements (Figure 4D). Altogether, our results indicate that, like PBs, AGs use the microtubule network to roam the cytoplasm. In addition, we observed that some AGs were in close contact with PBs, both in NPM-ALK–transfected NIH3T3 cells (Figures 2C and S3A) and ALCL-derived Cost-1 and Karpas cell lines (Figure S3B and unpublished data). To further analyze their interaction, we used NIH3T3 cells simultaneously transfected with

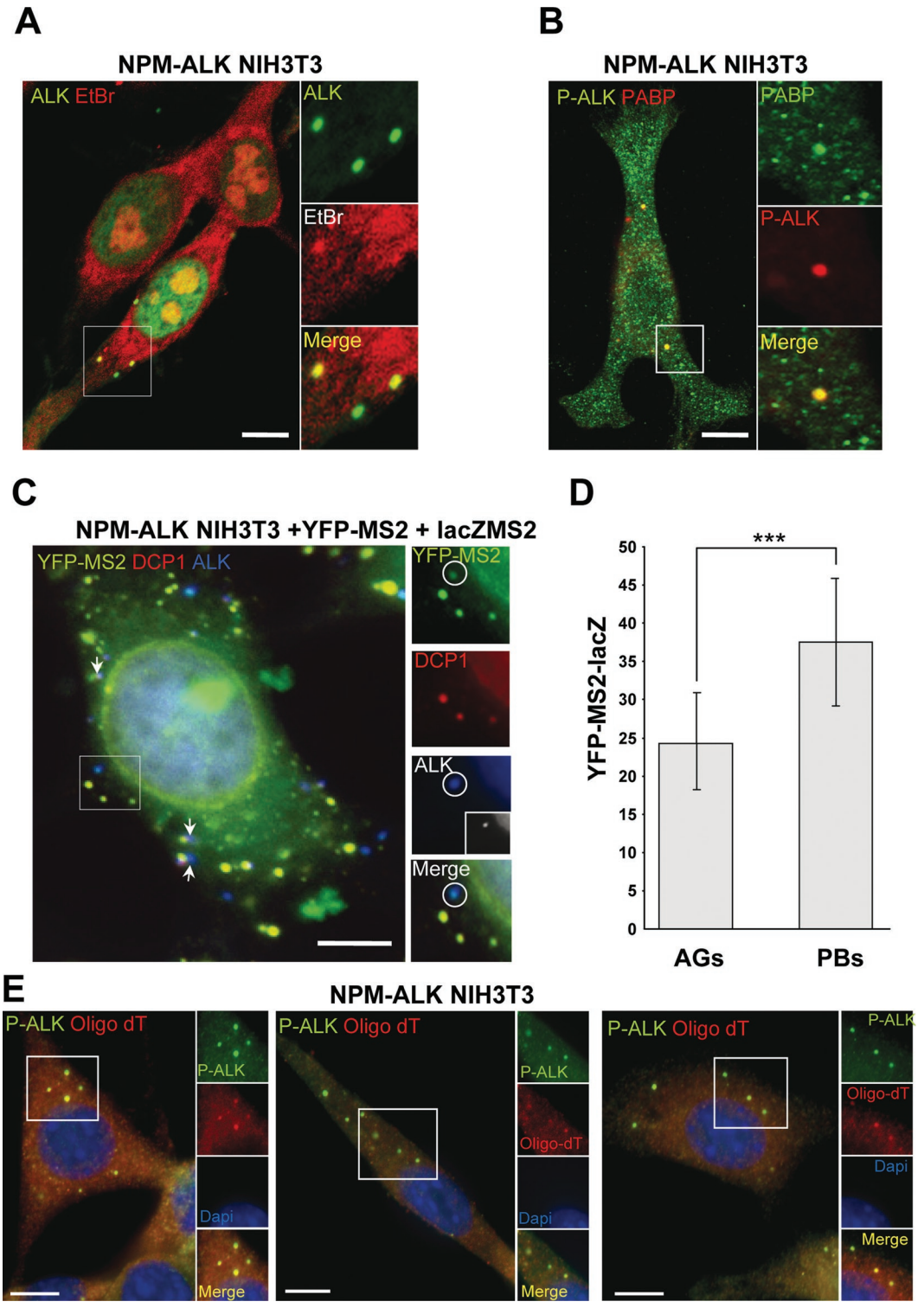

FIGURE 2: AGs contain mRNAs. (A) Stably NPM-ALK–expressing NIH3T3 cells were labeled with EtBr, stained with anti-ALK antibody, and analyzed by confocal microscopy to visualize AGs. (B) NPM-ALK–expressing NIH3T3 cells were doubly stained with anti-phospho-ALK (red) and anti-PABP (green) antibodies and analyzed by confocal microscopy. The yellow spots (merge) indicate that AGs contain PABP. (C) Cells transiently expressing MS2-lacZ mRNA and YFP-nls-MS2 fusion protein were analyzed by confocal microscopy to visualize PBs labeled with anti-hDCP1 (red in the enlarged square) and AGs labeled with anti-ALK antibodies (blue). In a small percentage of cells (2–5%), both granules contain the tethered reporter mRNAs (in the merge view, green (YFP) + red (hDCP1) = yellow; green (YFP) + blue (ALK) = cyan). Arrows show juxtaposed PBs and AGs. The scale bar in A–C represents 5 μm. (D) Intensity of YFP-MS2 signals was quantified in >50 AGs (cyan) and 50 PBs (yellow). Error bars represent standard deviation. ***$p < 0.001$. (E) In situ hybridization was performed to test the presence of polyadenylated mRNAs within AGs. Oligo(dT) probe (red) concentrates within AGs that are detected by immunofluorescence using anti-phospho-ALK antibodies (green). The merge picture shows that most AGs concentrate polyadenylated mRNAs (yellow).

NPM-ALK-Halo and GFP-DCP1 constructs and observed that AGs and PBs are tethered together for up to 30 min (Figure 5, Figure S4C, and Supplemental Movie 2). These results show that AGs and PBs can establish stable contact that might rely on their association with the microtubule network.

AGs recruit PB components upon altered mRNA metabolism

Although AGs and PBs are distinct entities, they both concentrate mRNAs and RNA binding proteins. We thus ask whether, like PBs, AG composition could be modified upon treatment affecting mRNA metabolism. First, we used cycloheximide (CHX) and actinomycin D (ActD), two drugs that reduce the pool of cytoplasmic mRNPs, leading to PB disaggregation (Cougot *et al.*, 2004 and Figure 6, G and H). None of these treatments induce change in AG number or size in comparison to untreated cells (see Figures 6A and 7 for quantification). Moreover, CHX treatment does not prevent polyA mRNA accumulation in AGs, as revealed by colocalization of oligo(dT) and NPM-ALK within AGs (Figure 6I). Remarkably, simultaneous detection of NPM-ALK and PB markers (DCP1, EDC3, LSM1, XRN1) revealed that 30% and 70% of AGs contain PB components, except XRN1, after treatment with CHX or ActD, respectively (Figures 6 and 7). In addition, whatever the treatment, most foci (94%) containing DCP1 also contain NPM-ALK (Figure 7, DCP1/ALK overlap). We also followed association of AGs and PBs by time-lapse using cells expressing NPM-ALK-GFP and RFP-RCK/p54, another component of PBs (reviewed in Kulkarni *et al.*, 2010) that does not produce artefacts when overexpressed (Mollet *et al.*, 2008). When those cells were treated with CHX, PBs and AGs gradually increased their contact and ultimately fused (Supplemental Movie 3). Relocalization of PB markers into AGs does not require complete PB disassembly because it is also observed after treatment with puromycin, a drug that does not dramatically prevent PB assembly (Figure 7). All together, these results show that treatments decreasing the pool of mRNAs do not affect nucleation of AGs but lead to the capture of PB components within AGs with the noticeable exception of XRN1.

AGs are distinct from SGs

AGs share some components with SGs, in particular mRNAs, PABP, and several AU-BPs (Buchan and Parker, 2009), such as HuR (M. Fawal, unpublished data). Thus, we wondered whether AGs could correspond to SG-like foci formed in NPM-ALK-transformed cells. We first tested whether known components of SGs, such as markers of the 40S subunit (ribosomal protein S6), translation initiation factors eIF2 and eIF3, and TIA/TIAR (Kedersha *et al.*, 2002, 2005) were present in AGs. Confocal analysis revealed that none of them are present in AGs in normal cell culture conditions (Figure 8, A and B, left panels, and unpublished data). Then, we asked whether stresses known to induce SGs could force accumulation of SG components within AGs. Neither heat shock (HS) nor arsenite treatment led to accumulation of TIAR or translation initiation factors (eIF2α or eIF3) in AGs, whereas those factors did concentrate within SGs (Figure 8, A and B), showing that AGs are distinct from SGs. This result was confirmed by overexpressing G3BP that leads to SG formation (Tourriere *et al.*, 2003). Immunostaining using anti-G3BP, anti-DCP1a, and anti-ALK antibodies to mark SGs, PBs, and AGs, respectively, revealed that all three types of granules were distinct entities (Figure 8C). All together, these results show that AGs do not accumulate known components of SGs in NPM-ALK NIH3T3 cells either in normal cell culture conditions or after various stresses and are thus different from SGs in essence.

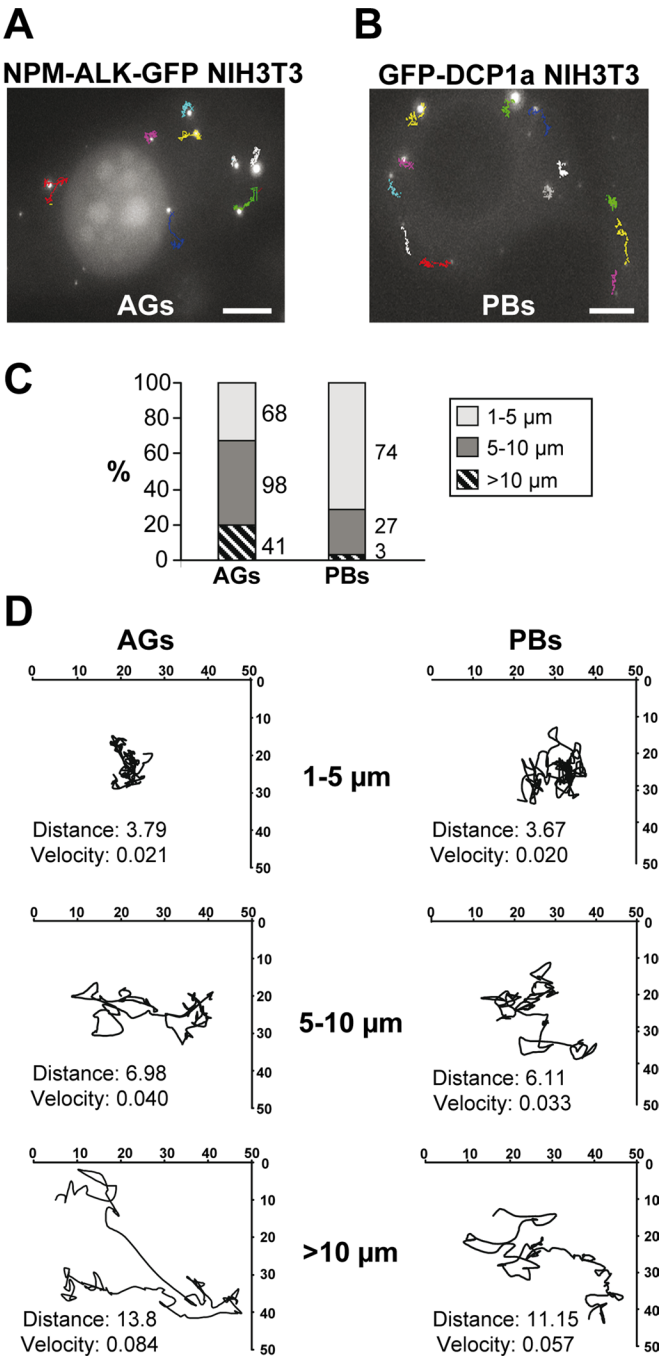

FIGURE 3: AG dynamics resembles that of PBs. (A and B) NIH3T3 cells were transiently transfected with an NPM-ALK-GFP (A) or GFP-DCP1a (B) expressing vector and observed by video microscopy. Representative images collected from 60 frames (total 2 min) showing tracks of multiple AGs (A) and PBs (B) are shown. (C) Tracks of ~200 AGs and 100 PBs were analyzed and divided into three categories following their roamed distances, <5 µm, 5–10 µm, or >10 µm. For a given category, mean distances and velocities (expressed in $\mu m^2/s$) are also indicated. The percentage of AGs or PBs belonging to a given category is shown. (D) Examples for each category of track and relative area (in pixels) in which AGs or PBs moved are given.

DISCUSSION

In this study, we have further characterized AGs, which are cytoplasmic bodies different from PBs and SGs. AGs were observed in ALCLs (Fawal *et al.*, 2006; Honorat *et al.*, 2006; this study) as well as

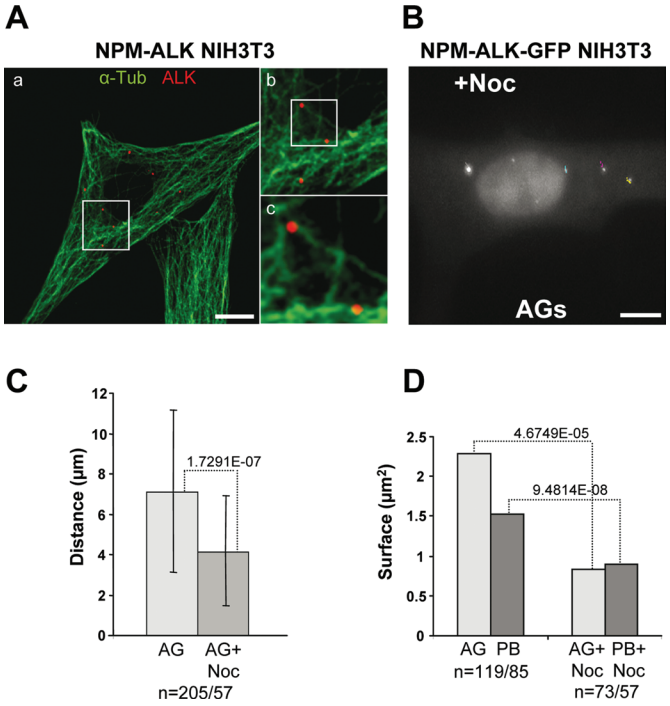

FIGURE 4: AGs reside on microtubules. (A) NPM-ALK NIH3T3 cells were doubly stained with anti–tubulin (green) and anti–ALK (red) antibodies and observed by confocal microscopy. a,b,c: successive enlargements. The scale bar represents 5 µm. (B) NIH3T3 cells transiently transfected with a NPM-ALK-GFP construct were treated with nocodazole for 30 min. Fresh medium was added, and AG movements were subsequently observed by video microscopy, as described in Figure 3, B and C, and their tracks were drawn. (C) Comparative analysis of the distances (in µm) crossed by AGs before and after nocodazole treatment. Error bars (standard deviations) and Student's *t* test values are indicated on each graph. (D) Comparative analysis of the surfaces (in square micrometers) roamed by PBs and AGs before and after nocodazole treatment. n indicates the number of AGs or PBs counted in each experiment. Student's *t* test values are indicated on each graph.

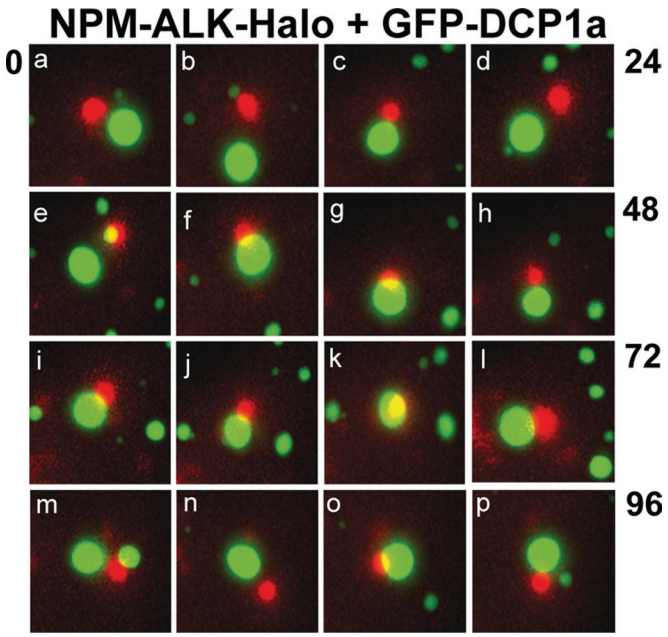

FIGURE 5: Close contacts between AGs and PBs. Live imaging of PB and AG communication. NIH3T3 cells were transiently cotransfected with NPM-ALK-Halo (red) and GFP-DCP1 (green) encoding plasmids. Two days later, cells were observed by wide-field microscopy, and time-lapse analysis was performed for two consecutive hours. Images taken every 6 min from 0 (a) to 96 min (p) on a region of contact are shown.

in the murine NIH3T3 cell line model expressing the NPM-ALK translocation (Fawal *et al.*, 2006) or other X-ALK fusion proteins (this study). We show that AG nucleation is independent of the N-terminal partner of the fusion protein as AGs are found in NPM-, ATIC-, or TPM3-ALK–expressing cells. The N-terminal part, however, promotes dimerization and allows ALK fusion kinases to transphosphorylate themselves (Chiarle *et al.*, 2008) and is thus indirectly required for AG formation. By contrast, cells expressing full-length ALK protein do not harbor AGs, possibly because the receptor, during its trafficking, is addressed to different subcellular compartments and/or forms holo- or heterocomplexes with a different subset of adaptor proteins.

As revealed by time-lapse analysis, AGs are rapidly formed and move in the cytoplasm. They decorate the microtubule network, and their movement is reduced upon microtubule depolymerization, indicating that their mobility relies on an intact microtubule network. Whether AG/microtubule association is direct, however, remains to be investigated. We compared AG to PB mobility in the same cellular context and found that their track patterns are similar, although the proportion of fast moving AGs is higher than that of mobile PBs. The distances roamed by PBs during the same given time (2 min) are in the same range as those reported by Aizer and Shav-Tal (2008) (2–10 µm), indicating that PB movements are comparable in the murine fibroblastic NIH3T3 cells and the human osteosarcoma U20S line (Aizer *et al.*, 2008). The velocity values are different, however, in the two studies; this discrepancy is most probably caused by different methods of measurements (see *Materials and Methods*).

A model has recently been proposed integrating polysomes, SGs, and PBs into an mRNP cycle that relies on the microtubule network (Buchan and Parker, 2009). The association of AGs with microtubules, as well as the presence in these foci of mRNA (this study) and two RNA-binding proteins, AUF1 (Fawal *et al.*, 2006) and HuR (unpublished data), suggest that AGs could also participate in the mRNP cycle. In normal cell culture conditions, AGs contain PABP and polyadenylated mRNAs, but not PB components. This indicates that by contrast to PBs, mRNAs concentrated in AGs are not engaged in a degradation process but are still competent for translation. AGs, however, do not concentrate components of the translation machinery or ribosomal subunits, indicating that the mRNAs stored or trafficking in AGs are most probably not stalled in the process of translation initiation, like those accumulating within SGs (reviewed in Buchan and Parker, 2009). Thus AGs may trap translatable mRNAs away from the decay machineries. As we frequently observed close contacts between AGs and PBs, these mRNAs could be captured from nearby PBs. The fact that AGs, but not PBs, concentrate polyadenylated mRNAs is not in agreement with this hypothesis but rather suggests that mRNAs contained in AGs are captured from the cytosol. In addition, PB components are not normally concentrated within AGs, although cells contain a diffuse cytoplasmic pool of those components (Mollet *et al.*, 2008 and reviewed in Aizer and Shav-Tal, 2008). Nevertheless, after treatments that alter mRNA metabolism, some PB components (LSM1, EDC3, RCK/p54, or DCP1a) are recruited in AGs. They might be captured from adjacent dissociating PBs, as suggested from video-microscopic observations. XRN1 does not, however, relocate to AGs during those

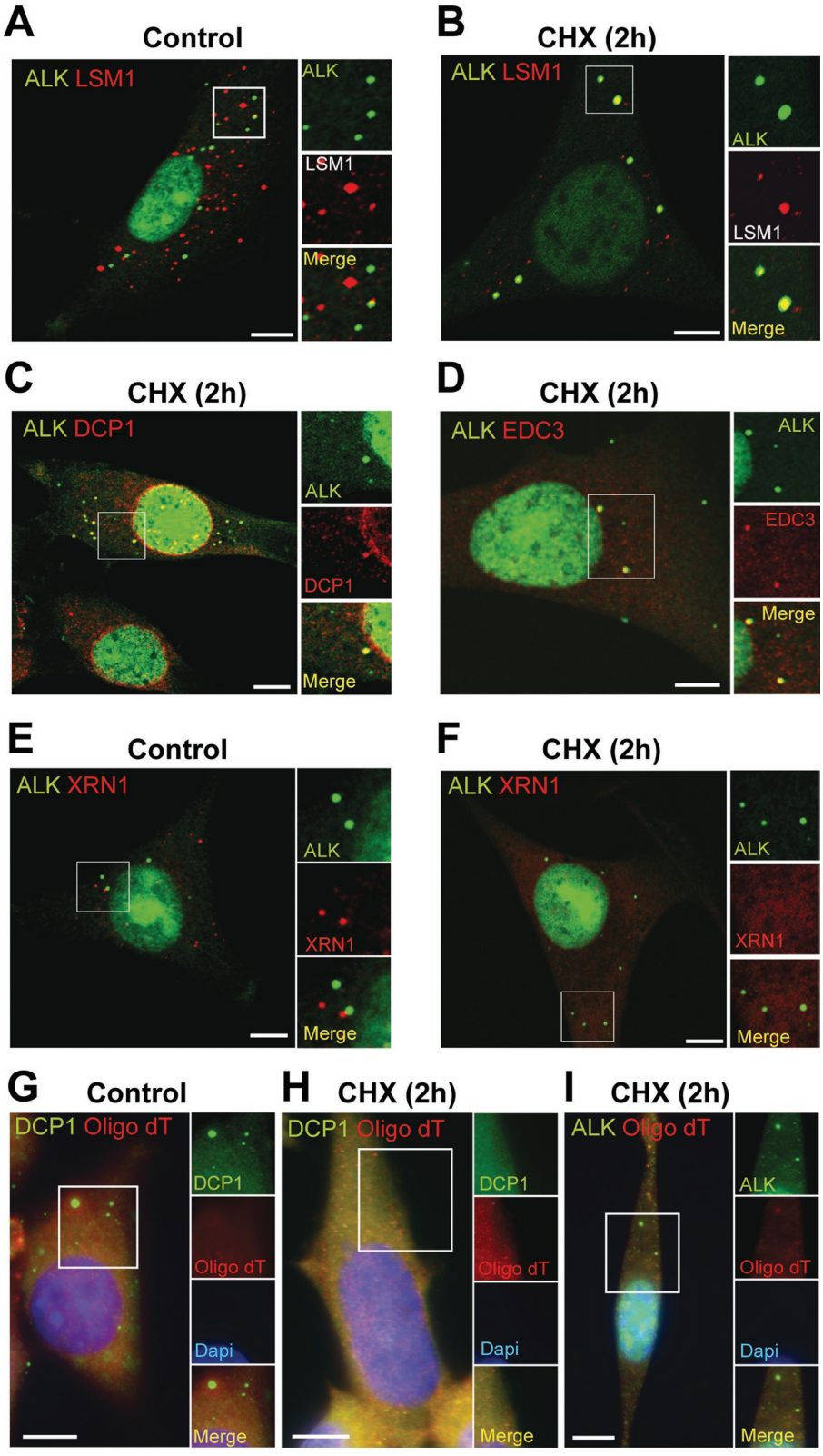

FIGURE 6: AGs and PBs share components when mRNA metabolism is altered. (A–F) NPM-ALK–expressing NIH3T3 cells were either untreated (A and E) or treated with CHX for 2 h (B–D, F). CHX treatment led to expression of LSM1 (B), DCP1 (C), EDC3 (D), but not XRN1 (F), within AGs. Representative images of cells containing more than three AGs and in which the size of PBs is >0.4 μm are shown. Such cells represent ~5% of a given field. Scale bar: 5 μm. G–I. NPM-ALK–expressing NIH3T3 cells were either untreated (G) or treated with CHX for 2 h (H and I). The presence of polyadenylated mRNAs within PBs or AGs was analyzed through in situ hybridization using oligo(dT) probe (red) and concomitant immunofluorescence study using anti-DCP1 (G and H) or anti-ALK antibodies (I) (green), respectively. Scale bar: 10 μm.

treatments, showing that, if it really takes place, relocalization of components from PBs to AGs is a selective process.

All together our data demonstrate that AGs are different from PBs and SGs and thus most probably do not act like PBs or SGs whose functions, despite an abundant literature, are still under debate (Franks and Lykke-Andersen, 2008; Mollet *et al.*, 2008; Balagopal and Parker, 2009; Buchan and Parker, 2009; Kulkarni *et al.*, 2010). It is thought that PBs roam the cytoplasm to collect mRNAs destined for degradation (Aizer and Shav-Tal, 2008), whereas SGs transiently store mRNAs engaged in the initiation step of translation. In SGs, arrested mRNAs are maintained intact (i.e., in their translatable state) until translation resumes. As AGs do not contain components of the translation machinery but are capable of sheltering polyadenylated mRNAs that are not tagged for degradation, we propose that, through their ability to scan the cytoplasm, AGs capture polyadenylated mRNAs that they will store away from degradation. Because ARE-containing mRNAs have been found stabilized in NPM-ALK–expressing cells (Fawal *et al.*, 2006), AGs could function as nursery for these mRNAs, allowing their dressing with AU-BPss, such as HuR or AUF1.

To conclude, we have described in this article mRNP cytoplasmic granules that are encountered in X-ALK–transformed cells in which simultaneous activation of various ALK-mediated signaling pathways dramatically enhances transcription (reviewed in Pulford *et al.*, 2004b). Permanent transcriptional activation might lead to mRNA influx that exceeds the translational capacity of these transformed cells. We would like to speculate that AGs constitute a reservoir system for translatable mRNAs that would have been degraded otherwise. Continuous availability for translation of some specific mRNAs with altered turnover could be the basis of the oncogenic properties of X-ALK–expressing cells. Whether and how mRNAs are sorted before storage in AGs are important questions for future studies.

MATERIALS AND METHODS

Cell culture

X-ALK stably transfected NIH3T3 cells and ALCLs-derived cell lines have been described (Armstrong *et al.*, 2004; Falini *et al.*, 1999). ActD (2 μg/ml final concentration), CHX (5 μg/ml), puromycin (20 μg/ml), and nocodazole (40 μM) (all obtained from Sigma, St. Louis, MO) were added to cell culture medium for the indicated times. The ALK inhibitor (Racemic PF-2341066 [3-[1-(2,6-dichloro-3-fluoro-phenyl)-ethoxy]-5-(1-piperidin-4-yl-1H-pyrazol-4-yl)-pyridin-2-ylamine) that resulted in the abolition of

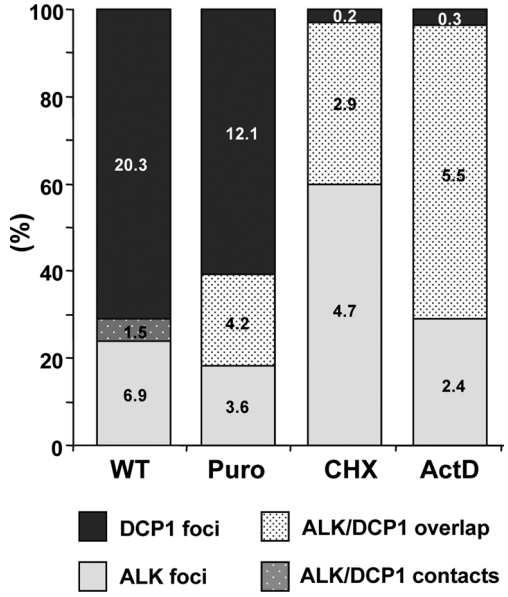

FIGURE 7: Merging of AGs and PBs. NPM-ALK NIH3T3 cells were doubly stained with anti-DCP1 and anti-ALK antibodies and observed under wide-field microscope. Foci that contained only DCP1 (PBs) or NPM-ALK (AGs) or both proteins (AG-PBs) were counted in untreated NPM-ALK NIH3T3 cells (WT) or after CHX or ActD (ActD) treatment that resulted in a decreased cytoplasmic pool of mRNAs and subsequently a nearly compete loss of PBs. By contrast, puromycin (Puro) that inhibits translation by the release of mRNA from polyribosomes does not inhibit PB formation to the same extent. Numbers in the graphs represent the average foci number for each category. Results shown were obtained in at least two independent experiments, and >100 cells were analyzed.

NPM-ALK autophosphorylation was synthesized according to the method described in the patent international application WO 2006/021881 and was used at a final concentration of 10^{-5} M.

Plasmids and transfection

GFP-ALK and ALK-Halo vectors were generated by cloning the full open reading frames of human NPM-ALK into *Hin*dIII/*Eco*RI sites of the EGFP (enhanced green fluorescent protein) N3 vector (Clontech, Mountain View, CA) or *Hin*dIII/*Eco*RV sites of Halotag pHT2 vector (Promega, Madison, WI). βgal MS2 (RSV-Z-MS2–24), YFP-MS2 (L_{30}-YFP-$MS2_{nls}$), GFP-DCP1, and RFP-RCK/p54 were gifts from E. Bertrand (IGMM)–UMR5535, Montpellier, France), B. Seraphin (IGBMC, Strasbourg, France), and D. Weil (CNRS FRE2937, IAL, Villejuif, France). NIH3T3 cells were transiently transfected using Lipofectamine following the manufacturer's instructions (Invitrogen, Carlsbad, CA). Double transfections were done with a 1:1 ratio, except for YFP-MS2/LacZ-MS2–24, which was performed with a ratio of 1:10. NIH3T3 cells stably transfected with full-length ALK complementary DNA were provided by I. Janoueix and O. Delattre (Institut Curie, Paris, France).

Immunofluorescence and live cell imaging

For immunofluorescence analysis, NIH3T3 cells were seeded on glass coverslips (10^4 cells/ml), cultured overnight, fixed, permeabilized, and stained as described (Fawal *et al.*, 2006). The antibodies used were as follows: monoclonal anti-ALK1 (DakoCytomation, Carpinteria, CA), rabbit anti-phospho-ALK (Cell Signalling Technologies, Beverly, MA), rabbit anti-hDCP1a (gift from B. Séraphin, IGBMC, Strasbourg, France), anti-Edc3 and anti-Xrn1 (gift from J. Lykke-Andersen, University of Colorado, USA), and anti-PABP (Sigma). The secondary antibodies were goat anti–rabbit antibody (Alexa 566; Molecular Probes) or goat anti–mouse (Alexa 488; Molecular Probes). Slides were mounted in Mowiol and analyzed with a Leica SP2 confocal microscope equipped with helium-neon lasers and appropriate filter combinations or a wide-field Leica DMIRE2 microscope equipped with a micromax Princeton CCD camera. Unless otherwise specified, all images are single Z sections from a series of confocal images. The images were acquired using Leica or MetaMorph software (Universal Imaging) and edited with Adobe Photoshop.

For time-lapse analysis, NIH3T3 cells were seeded on Nunc (Rochester, NY) 4-cm glass-bottom dishes. Cells were transfected as described earlier in text and observed 36-48 h posttransfection. Cells were maintained at 37°C and 5% CO_2, and signals were detected by a Leica DMIRE 2 microscope driven by MetaMorph software. A 63× oil-immersion inversed objective was used. Images were acquired every 6 min and represent the maximal projection of 14 planes with 0.16-μm optical sections. For short-range movies, images were acquired every 2 s and represent a maximal projection of 7 planes with 0.16-μm optical sections. For statistical analysis, the distance of granules (AGs and PBs) were measured on a minimum of 100 granules from at least 15 different cells per movie using MetaMorph software utility, Track objects. Tracks were recorded. ImageJ was used to calculate the area corresponding to the best fit ellipse covered by a given track. To calculate velocity, we divided the distance roamed during the time of observation (2 min plus the time for collecting data between sections). In the study by Aizer and collaborators, instantaneous velocities were reported on the basis of total distance and mean square displacements that allow the calculation of diffusion coefficients (Aizer *et al.*, 2008).

Detection of polyadenylated mRNAs within AGs

NPM-ALK 3T3 cells seeded on glass coverslips were incubated 15 min in paraformaldehyde 4% and 5 min in 0.1% Triton X-100, rinsed in phosphate-buffered saline, and incubated 30 min in 2× (SSC)/50% formamide. Polyadenylated mRNAs contained in AGs were detected by in situ hybridization using a digoxigenin-labeled DNA oligo(dT) probe. Hybridization of 50 ng of oligo(dT) probe was performed in 50 μl of hybridization solution (2× SSC/50% formamide/10% dextran sulfate/0.5 mg/ml yeast tRNA/Rnase inhibitor; Promega) at 37°C overnight. Cells were then washed twice for 30 min in 2× SCC/50% formamide at 37°C and 20 min in 1× SSC. Oligo(dT) signal was detected using anti-digoxigenin sheep antibodies that were recognized by donkey anti–sheep antibodies (Alexa 654; Molecular Probes). AGs were detected using either anti-ALK or anti–phospho-ALK antibodies that were incubated together with the anti-digoxigenin antibodies. Cells were analyzed under a wide field microscope, and images were treated using Adobe Photoshop.

ACKNOWLEDGMENTS

We thank J. Smith for critical reading of the manuscript. We are grateful to B. Ronsin and A. Le Ru for their help with confocal and live image analysis (Imagery plateform of Toulouse). We thank the Delsol laboratory for X-ALK–transfected cells and ALCL-derived cell lines, and we express gratitude to Prof. G. Delsol for his unfailing support. This work was supported by ARC (Association pour la Recherche contre le Cancer) contracts 3823 (DM) and 4891 (OJ-J), ARECA network Pôle protéomique et Cancer, Conseil Régional "Cibles thérapeutiques et recherche de nouveaux marqueurs diagnostics et pronostics dans les cancers," and La Ligue Contre le Cancer. M. Fawal was supported by an ARC fellowship.

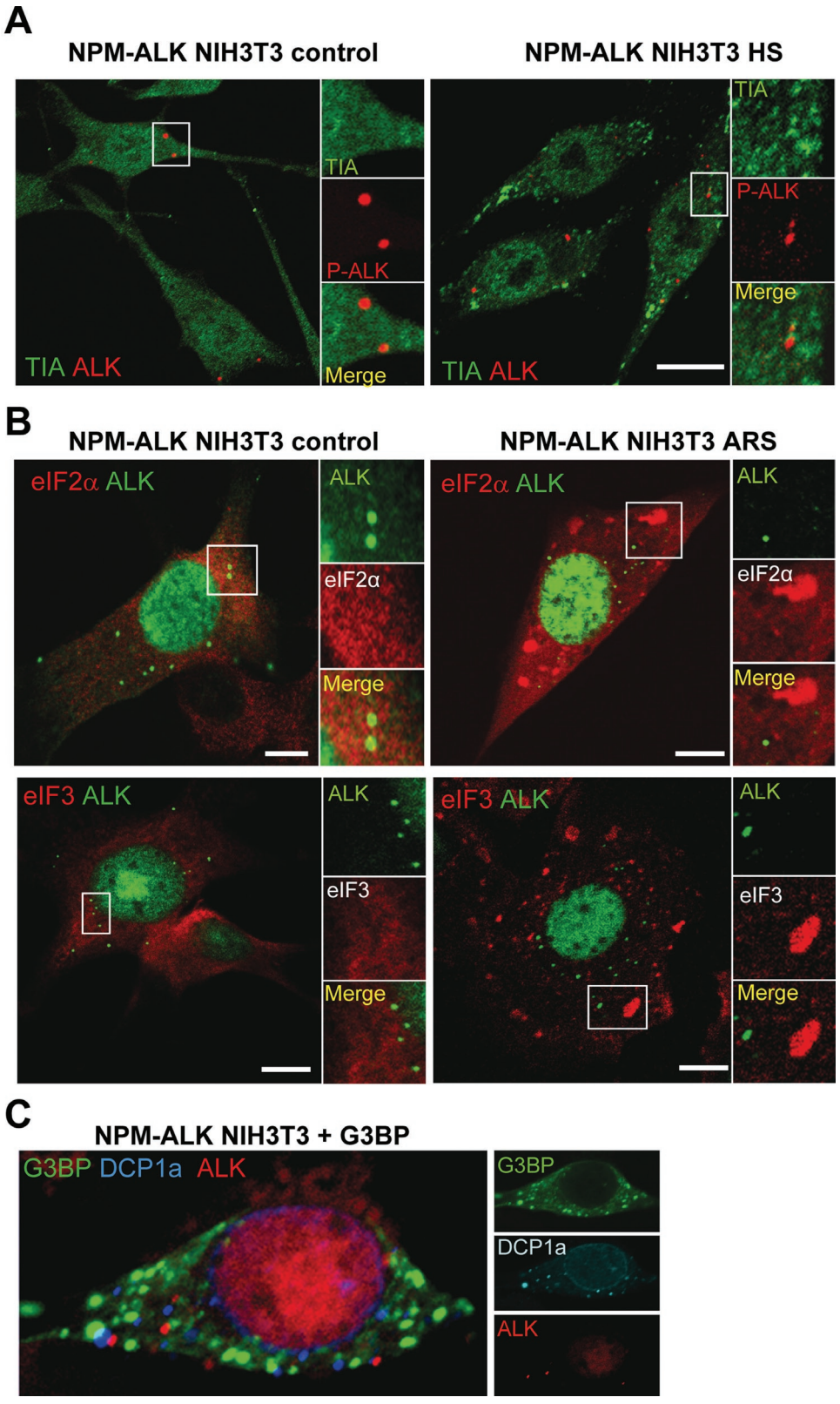

FIGURE 8: AGs and SGs are two independent structures. (A and B). NPM-ALK–expressing NIH3T3 cells were untreated (control), heat shocked (HS) (44°C for 30 min), or treated with arsenite (ARS) for 2 h to induce SGs. Confocal analysis was undertaken to visualize TIA, eIF2α, or eIF3 in AGs or SGs using concomitantly anti–phospho-ALK antibody to label AGs. In the absence of stress, we observed punctuate cytoplasmic labeling of eIF2α or eIF3 in control NPM-ALK cells, but no specific labeling of AGs by these proteins. HS and ARS treatment induced the formation of SGs, revealed by TIA concentration in SGs in control and NPM-ALK–expressing cells but not in AGs visualized by accumulation of phospho-ALK protein. (C) SGs were induced by transient GFP-G3BP overexpression in NPM-ALK–expressing cells. SGs, PBs, and AGs were simultaneously observed by confocal analysis using GFP fluorescence, anti-DCP1 antibodies, and anti–ALK antibodies, respectively.

REFERENCES

Aizer A, Brody Y, Mer LW, Sonenberg N, Singer RH, Shav-Tal Y (2008). The dynamics of mammalian P body transport, assembly, and disassembly in vivo. Mol Biol Cell 19, 4154–4166.

Anderson P, Kedersha N (2009). RNA granules: posttranscriptional and epigenetic modulators of gene expression. Nat Rev Mol Cell Biol 10, 430–436.

Anderson P, Kedersha N (2008). Stress granules: the Tao of RNA triage. Trends Biochem Sci 33, 141–150.

Armstrong F *et al*. (2004). Differential effects of X-ALK fusion proteins on proliferation, transformation, and invasion properties of NIH3T3 cells. Oncogene 23, 6071–6082.

Bai RY, Ouyang T, Miething C, Morris SW, Peschel C, Duyster J (2000). Nucleophosmin-anaplastic lymphoma kinase associated with anaplastic large-cell lymphoma activates the phosphatidylinositol 3-kinase/Akt antiapoptotic signaling pathway. Blood 96, 4319–4327.

Balagopal V, Parker R (2009). Polysomes, P bodies and stress granules: states and fates of eukaryotic mRNAs. Curr Opin Cell Biol 21, 403–408.

Benharroch D *et al*. (1998). ALK-positive lymphoma: a single disease with a broad spectrum of morphology. Blood 91, 2076–2084.

Bevilacqua A, Ceriani MC, Capaccioli S, Nicolin A (2003). Post-transcriptional regulation of gene expression by degradation of messenger RNAs. J Cell Physiol 195, 356–372.

Bhattacharyya SN, Habermacher R, Martine U, Closs EI, Filipowicz W (2006). Stress-induced reversal of microRNA repression and mRNA P-body localization in human cells. Cold Spring Harb Symp Quant Biol 71, 513–521.

Brengues M, Teixeira D, Parker R (2005). Movement of eukaryotic mRNAs between polysomes and cytoplasmic processing bodies. Science 310, 486–489.

Buchan JR, Parker R (2009). Eukaryotic stress granules: the ins and outs of translation. Mol Cell 36, 932–941.

Chernov KG, Barbet A, Hamon L, Ovchinnikov LP, Curmi PA, Pastre D (2009). Role of microtubules in stress granule assembly: microtubule dynamical instability favors the formation of micrometric stress granules in cells. J Biol Chem 284, 36569–36580.

Chiarle R, Voena C, Ambrogio C, Piva R, Inghirami G (2008). The anaplastic lymphoma kinase in the pathogenesis of cancer. Nat Rev Cancer 8, 11–23.

Cougot N, Babajko S, Seraphin B (2004). Cytoplasmic foci are sites of mRNA decay in human cells. J Cell Biol 165, 31–40.

Duyster J, Bai RY, Morris SW (2001). Translocations involving anaplastic lymphoma kinase (ALK). Oncogene 20, 5623–5637.

Eulalio A, Behm-Ansmant I, Izaurralde E (2007). P bodies: at the crossroads of posttranscriptional pathways. Nat Rev Mol Cell Biol 8, 9–22.

Falini B *et al*. (1999). Lymphomas expressing ALK fusion protein(s) other than NPM-ALK. Blood 94, 3509–3515.

Fawal M, Armstrong F, Ollier S, Dupont H, Touriol C, Monsarrat B, Delsol G, Payrastre B, Morello D (2006). A "liaison dangereuse" between AUF1/hnRNPD and the oncogenic tyrosine kinase NPM-ALK. Blood 108, 2780–2788.

Fenger-Gron M, Fillman C, Norrild B, Lykke-Andersen J (2005). Multiple processing body factors and the ARE binding protein TTP activate mRNA decapping. Mol Cell 20, 905–915.

Franks TM, Lykke-Andersen J (2007). TTP and BRF proteins nucleate processing body formation to silence mRNAs with AU-rich elements. Genes Dev 21, 719–735.

Franks TM, Lykke-Andersen J (2008). The control of mRNA decapping and P-body formation. Mol Cell 32, 605–615.

Gallouzi I, Brennan C, Stenberg M, Swanson M, Eversole A, Maizels N, Steitz J (2000). HuR binding to cytoplasmic mRNA is perturbed by heat shock. Proc Natl Acad Sci USA 97, 3073–3078.

Garneau NL, Wilusz J, Wilusz CJ (2007). The highways and byways of mRNA decay. Nat Rev Mol Cell Biol 8, 113–126.

Grummitt CG, Townsley FM, Johnson CM, Warren AJ, Bycroft M (2008). Structural consequences of nucleophosmin mutations in acute myeloid leukemia. J Biol Chem 283, 23326–23332.

Honorat JF, Ragab A, Lamant L, Delsol G, Ragab-Thomas J (2006). SHP1 tyrosine phosphatase negatively regulates NPM-ALK tyrosine kinase signaling. Blood 107, 4130–4138.

Kedersha N, Chen S, Gilks N, Li W, Miller IJ, Stahl J, Anderson P (2002). Evidence that ternary complex (eIF2-GTP-tRNA(i)(Met))-deficient preinitiation complexes are core constituents of mammalian stress granules. Mol Biol Cell 13, 195–210.

Kedersha N, Stoecklin G, Ayodele M, Yacono P, Lykke-Andersen J, Fritzler MJ, Scheuner D, Kaufman RJ, Golan DE, Anderson P (2005). Stress granules and processing bodies are dynamically linked sites of mRNP remodeling. J Cell Biol 169, 871–884.

Kedersha NL, Gupta M, Li W, Miller I, Anderson P (1999). RNA-binding proteins TIA-1 and TIAR link the phosphorylation of eIF-2 alpha to the assembly of mammalian stress granules. J Cell Biol 147, 1431–1442.

Kiebler MA, Bassell GJ (2006). Neuronal RNA granules: movers and makers. Neuron 51, 685–690.

Kulkarni M, Ozgur S, Stoecklin G (2010). On track with P-bodies. Biochem Soc Trans 38, 242–251.

Lamant L, Dastugue N, Pulford K, Delsol G, Mariame B (1999). A new fusion gene TPM3-ALK in anaplastic large cell lymphoma created by a (1;2)(q25;p23) translocation. Blood 93, 3088–3095.

Mollet S, Cougot N, Wilczynska A, Dautry F, Kress M, Bertrand E, Weil D (2008). Translationally repressed mRNA transiently cycles through stress granules during stress. Mol Biol Cell 19, 4469–4479.

Morris SW, Naeve C, Mathew P, James PL, Kirstein MN, Cui X, Witte DP (1997). ALK, the chromosome 2 gene locus altered by the t(2;5) in non-Hodgkin's lymphoma, encodes a novel neural receptor tyrosine kinase that is highly related to leukocyte tyrosine kinase (LTK). Oncogene 14, 2175–2188.

Moser JJ, Fritzler MJ (2010). Cytoplasmic ribonucleoprotein (RNP) bodies and their relationship to GW/P bodies. Int J Biochem Cell Biol 42, 828–843.

Nadezhdina ES, Lomakin AJ, Shpilman AA, Chudinova EM, Ivanov PA (2010). Microtubules govern stress granule mobility and dynamics. Biochim Biophys Acta 1803, 361–371.

Piecyk M *et al*. (2000). TIA-1 is a translational silencer that selectively regulates the expression of TNF-alpha. EMBO J 19, 4154–4163.

Pulford K, Lamant L, Espinos E, Jiang Q, Xue L, Turturro F, Delsol G, Morris SW (2004a). The emerging normal and disease-related roles of anaplastic lymphoma kinase. Cell Mol Life Sci 61, 2939–2953.

Pulford K, Lamant L, Morris SW, Butler LH, Wood KM, Stroud D, Delsol G, Mason DY (1997). Detection of anaplastic lymphoma kinase (ALK) and nucleolar protein nucleophosmin (NPM)-ALK proteins in normal and neoplastic cells with the monoclonal antibody ALK1. Blood 89, 1394–1404.

Pulford K, Morris SW, Turturro F (2004b). Anaplastic lymphoma kinase proteins in growth control and cancer. J Cell Physiol 199, 330–358.

Rook MS, Lu M, Kosik KS (2000). CaMKIIalpha 3' untranslated region-directed mRNA translocation in living neurons: visualization by GFP linkage. J Neurosci 20, 6385–6393.

Seydoux G, Braun RE (2006). Pathway to totipotency: lessons from germ cells. Cell 127, 891–904.

Sheth U, Parker R (2006). Targeting of aberrant mRNAs to cytoplasmic processing bodies. Cell 125, 1095–1109.

Tang SJ, Meulemans D, Vazquez L, Colaco N, Schuman E (2001). A role for a rat homolog of staufen in the transport of RNA to neuronal dendrites. Neuron 32, 463–475.

Teixeira D, Sheth U, Valencia-Sanchez MA, Brengues M, Parker R (2005). Processing bodies require RNA for assembly and contain nontranslating mRNAs. RNA 11, 371–382.

Touriol C, Greenland C, Lamant L, Pulford K, Bernard F, Rousset T, Mason DY, Delsol G (2000). Further demonstration of the diversity of chromosomal changes involving 2p23 in ALK-positive lymphoma: 2 cases expressing ALK kinase fused to CLTCL (clathrin chain polypeptide-like). Blood 95, 3204–3207.

Tourriere H, Chebli K, Zekri L, Courselaud B, Blanchard JM, Bertrand E, Tazi J (2003). The RasGAP-associated endoribonuclease G3BP assembles stress granules. J Cell Biol 160, 823–831.

Trinei M, Lanfrancone L, Campo E, Pulford K, Mason DY, Pelicci PG, Falini B (2000). A new variant anaplastic lymphoma kinase (ALK)-fusion protein (ATIC-ALK) in a case of ALK-positive anaplastic large cell lymphoma. Cancer Res 60, 793–798.

Wilczynska A, Aigueperse C, Kress M, Dautry F, Weil D (2005). The translational regulator CPEB1 provides a link between dcp1 bodies and stress granules. J Cell Sci 118, 981–992.

Zamo A, Chiarle R, Piva R, Howes J, Fan Y, Chilosi M, Levy DE, Inghirami G (2002). Anaplastic lymphoma kinase (ALK) activates Stat3 and protects hematopoietic cells from cell death. Oncogene 21, 1038–1047.

Zhang W, Wagner BJ, Ehrenman K, Schaefer AW, DeMaria CT, Crater D, DeHaven K, Long L, Brewer G (1993). Purification, characterization, and cDNA cloning of an AU-rich element RNA-binding Protein, AUF1. Mol Cell Biol 13, 7652–7665.